Mohamed Zaidan QAWAQZEH[1], Andrzej SZAFRANIEC[2], Serhii HALKO[3], Oleksandr MIROSHNYK[4], Anton ZHARKOV[3]

Al-Balqa Applied University, Jordan (1), University of Technology and Humanities in Radom (2),Tavria State Agrotechnological University (3), Kharkiv Petro Vasylenko National Technical University of Agriculture (4)

doi:10.15199/48.2020.11.08

Modelling of a household electricity supply system based on a wind power plant

Abstract. *A functional scheme of a household power supply system based on a low-power wind power plant with an electric generator excited by constant neodymium magnets is provided which supplies a given voltage level to the consumer in non-stationary stochastic dynamic modes characterized by random wind speed and loading magnitude. Mathematical modelling of its operating modes is performed and an adequate mathematical model describing stationary and transient processes in the proposed system is obtained.*

Streszczenie. *Przedstawiono schemat funkcjonalny układu zasilania gospodarstw domowych na bazie elektrowni wiatrowej małej mocy z prądnicą wzbudzaną przez stałe magnesy neodymowowe, który dostarcza konsumentom napięcie na danym poziomie w niestacjonarnych stochastycznych trybach dynamicznych, charakteryzujących się losową prędkością wiatru i wielkością ładunku. Podjęto matematyczne modelowanie jej trybów pracy, uzyskując odpowiedni model matematyczny opisujący procesy stacjonarne i przejściowe w proponowanym układzie.* ***(Modelowanie domowego układu zasilania energią elektryczną na bazie elektrowni wiatrowej)****.*

Keywords: renewable energy sources, wind power plants, energy conversion, energy storage batteries.
Słowa kluczowe: źródła energii odnawialnej, elektrownie wiatrowe, przemiany energii, baterie magazynujące energię.

Introduction

Wind power has been one of the fastest growing renewable energy sources in the last decade, providing about 3% of global electricity consumption [1, 2, 3].

The specific nature of small households is due to their relatively small electricity consumption and requires large-scale development of small wind power engineering, which, based on technical conditions, is limited to 10 kW. Research in the market for wind energy equipment shows that small consumers intend to use wind turbines to meet their needs (for example, power supply for industrial and household equipment, lighting, charging of automotive batteries, etc.) [4].

Wind power installations (WPI) convert kinetic energy of the wind into electricity. Stand-alone WPIs produce electricity for domestic and industrial needs and represent a modern alternative to traditional electricity supply [5].

The main element of a WPI is a wind wheel (WW). Potential for increasing a WW's rotational speed is limited by aerodynamic factors. Use of reducers and other mechanical devices for this purpose is inappropriate as additional energy losses emerge and overall dimensions deteriorate. In low-power plants, multipole generators on permanent magnets are most commonly used [5, 6, 7]. Generators on permanent magnets, which are simple in design, reliable, and do not require additional power for winding excitation, offer prospects in this connection.

WPIs need to work in conditions of variable wind speed, the individual impulses of which can significantly exceed average speed, while at other times the speed can drop significantly. This enforces application of complex mechanical or hydraulic speed control devices, which considerably complicates the whole structure and is unacceptable for autonomous low-power WPIs [8, 9, 10, 11]. It is better to use installations with intermediate direct current links and buffer storage of energy that can be subsequently transformed into industrial frequency voltage and current [5, 12]. Based on comparable characteristics of the generator and wind-wheel capacities, [13] recommendeds adjustments to the plant power in the generator excitation circuit, which is unacceptable for patented non-direct-current wind turbine generators on permanent magnets [6, 7].

Among the various types of energy storage devices, the most attractive means for buffer energy storage in low power plants are accumulators [14, 15], which are recharged at a sufficient wind speed and supply energy to the load when the wind speed falls and power shortages arise. It is expedient to apply a resistive ballast load, which receives excess power at high wind speeds [13], for operative regulation of power from a generator to a load.

Literature offers sufficiently developed typical circuits of large and medium power WPIs, as well as operation modes of generators with electromagnetic excitation or excitation from permanent magnets [5]. Non-stationary dynamic regimes of low power WPIs have been investigated. To a lesser extent, characterized by random wind speed and random load resistance, provided the voltage is stabilized at instantaneous values of the wind speed and output voltage of the generator.

The aim of this study is development of a functional scheme of a power supply system on the basis of a low power generator WPI with permanent magnets and simulation of its operation in conditions of random wind speed and random variation of load resistance.

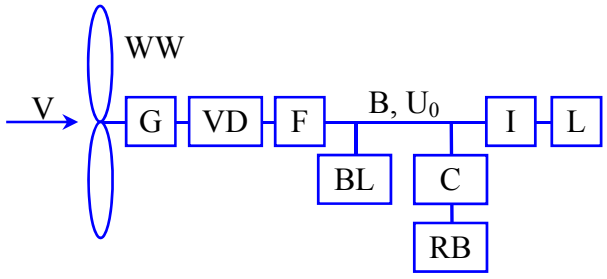

Fig.1. Functional scheme of a power supply system on the basis of WPI

Experimental

A functional scheme of the proposed power supply system with a low power WPI on an electric generator with permanent neodymium magnets is depicted in Fig. 1. The scheme works in the following way.

Phase voltage from the generator G connected to the uncontrolled rectifier bridge VD and through damping filter F enters the team bus B. It also connects a resistive ballast load BL and a rechargeable battery RB through the controller C «charge-discharge» of a battery. From the combined bus B, the voltage goes to the inverter, the output of which is the load L.

With an excess of generator power, which is expressed in a higher voltage caused by a greater wind speed V, conductivity of the ballast load BL increases, which leads to selection of excessive power. In addition, the rechargeable battery RB can be recharged in these conditions; its controller C provides charging current limitation and its full termination at maximum charge. As a result, the voltage on the combined bus B does not rise substantially. Something similar happens when power consumed by the load decreases. With a complete loss of load power L and a fully charged battery RB, the WW wind wheel is braked, for example, in the systems described in articles [16, 17]. Thus, the proposed system does not provide for mechanical control of the speed of the wind wheel WW; this is done by adjusting the load of the generator G.

Power shortages occur when the wind speed V is lower or with a load L on the inverter I. With a deficiency of power on the combined bus B and conductance BL down to zero, the battery pack RB, which is discharged, maintains voltage at a constant level. Controller C limits the discharge current of the rechargeable battery RB and protects it against the maximum allowable discharge. Conductivity of the ballast load BL is changed by connecting low resistors to the combined bus B through a frequency pulse width modulation device 4-6 kHz.

Results and discussion

A mathematical description of the operating modes of a generator with permanent magnets under the condition of a sinusoidal curve of the output voltage and of the unsaturated magnetic circuit is performed in orthogonal q coordinates with a forward rotation of the longitudinal axis. In such generators there are no special damping windings on the rotor; their role is played by massive parts of the rotor. According to [8], damping currents have relatively little influence on the mode of such a generator, so they are not considered further in the mathematical model. In addition, a change in the magnetic flux due to partial demagnetization is manifested only with currents close to the short circuit. Therefore, we further believe that the magnetic flux of magnets remains constant. It should be noted that such an assumption was made by developers of the model of a machine with permanent magnets in the package of imitation modelling MATLAB Simulink.

Thus, the equation for the longitudinal and transverse component of the currents and voltage of the generator has the following form [8]:

$$(1)\quad \begin{cases} 1{,}5ri_d + 1{,}5L_d\dfrac{di_d}{dt} + 1{,}5L_q i_q \Omega p + u_d = 0; \\ 1{,}5ri_q + 1{,}5L_q\dfrac{di_q}{dt} - 1{,}5L_d i_d \Omega p - 1{,}5\Psi\Omega p + u_q = 0, \end{cases}$$

where: i_d, u_d, i_q, – longitudinal and transverse components of phase voltages and currents at the output of the generator;
L_d, L_q – inductance of the phase winding of the generator stator along the corresponding axes,
p – the number of pairs of poles,
r – active resistance of the stator winding phase,
Ψ – magnetic flux in the longitudinal axis of the generator.

Neglecting the electric inertia of the generator windings in comparison with its mechanical inertia and considering the generalized load impedance R_L mainly resistive, we obtain the final equation:

$$(2)\quad \begin{cases} 1{,}5ri_d + 1{,}5L_q i_q \Omega p + \dfrac{1}{\sqrt{3}}R_L i_d = 0; \\ 1{,}5ri_q - 1{,}5L_d i_d \Omega p - 1{,}5\Psi\Omega p + \dfrac{1}{\sqrt{3}}R_L i_q = 0, \end{cases}$$

where:

$$(3)\ i_q = \frac{1{,}5\Psi\Omega p\left(1{,}5r + \dfrac{1}{\sqrt{3}}R_L\right)}{L_d L_q (1{,}5\Omega p)^2 + \left(1{,}5r + \dfrac{1}{\sqrt{3}}R_L\right)^2} = \frac{1{,}5\Psi\Omega p L_d L_q}{1{,}5r + \dfrac{1}{\sqrt{3}}R_L};$$

The equation of the dynamics of the WPI's mechanical part becomes an equation of equilibrium of moments:

$$(4)\quad \begin{aligned} J\frac{d\Omega}{dt} + k_{cf}\Omega + M_G &= M_{WW}; \\ M_G &= 1{,}5pi_q\left[1{,}5\Psi + (L_d - L_q)i_d\right], \end{aligned}$$

where: J – moment of inertia of rotating masses, k_{cf} – coefficient of friction, M_G – electromagnetic moment of the generator, M_{WW} – winding torque, which depends on the speed of its rotation and wind speed [5]:

$$(5)\quad M_{WW} = M(z)\frac{D^3\rho\pi V^3}{16},$$

where: D – diameter of the wind wheel, ρ – air density, $M(z)$ – relative moment of the wind wheel, which depends on the speed z.

A typical graph of the relative torque for a trilateral windrow, shown in Fig. 2 with the solid lines 1 [5].

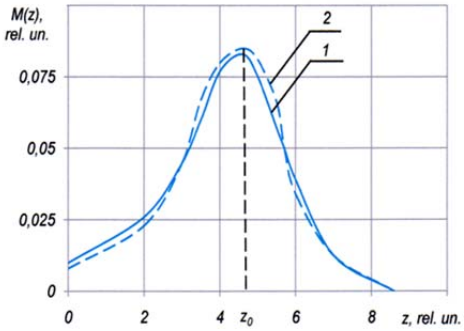

1 – typical; 2 – approximated for (6)

Fig.2. Dependencies of relative moment *M(z)* on high speed *z*

For modelling purposes, this moment is approximated by a nonlinear dependence

$$(6)\quad M(z) = k_1 e^{-k_2(z-z_0)^2} + k_3 e^{-k_4 z} + k_5 \sin z - k_6 z^5,$$

where: $k_1 - k_6$ – coefficients of approximation.

In Fig. 2, the approximated dependence (6) is shown by the dashed line 2 with the following parameter values: k_1 =0.09, k_2 =0.35, k_3 =0.006, k_4 =0.03, k_5 =0.009, k_6 =3·10^{-7}.

It follows from Fig. 2 the approximation sufficiently reflects the original curve, especially given that the original curve itself $M(z)$ is usually presented in a much averaged form [5].

The graph of the dependence of load resistance r_{BL} on voltage u across the combined bus B is depicted in Fig. 3. At a voltage greater than U_0, resistance r_{BL} decreases and the ballast load takes an excess of power, which stabilizes the tension on the combined bus B. When power is absent and the voltage reduces, the ballast load resistance r_{BL} increases. The dependence $r_{BL} = f(u)$ at $u > U_0$ in Fig. 3 is approximated by the expression:

$$(7)\quad r_{BL} = \frac{2}{u - U_0 + 0{,}002},$$

where: u – the current value of the voltage on the combined bus.

A partially linear approximation of the expression is also possible (7). When implementing the system, the law of high-frequency pulse-width modulation is constructed in such a way as to provide an average resistance value r_{BL} according to the curve (7).

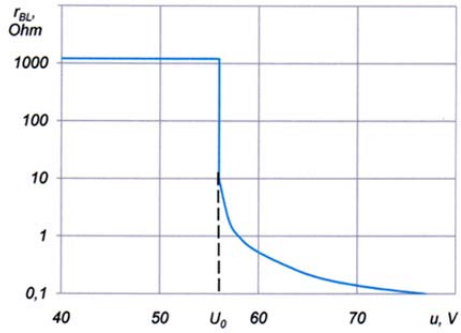

Fig.3. Dependence of r_{BL} load resistance on B bus voltage

An idealized voltage-ampere characteristic (VAC) of rechargeable battery $I = f(u)$ is depicted on Fig. 4 with the dashed line. The nearly vertical portion of this curve at $I > 0$ matches the charging mode and at $I < 0$ – the discharging mode. Horizontal areas are non-working and unacceptable; the battery controller precludes access to these areas, limiting the currents of charge and discharge almost to the vertical part of the characteristic.

Battery charge $g_{RB} = f(u)$ (the solid line in Fig. 4), corresponding to this VAC, is approximated by the expression:

$$(8)\qquad \begin{cases} g_{RB}(u) = \dfrac{b_1}{u} - \dfrac{b_2}{U_0} e^{-b_2(u-U_0)};\ u > U_0; \\ g_{RB}(u) = \dfrac{b_1}{u} - \dfrac{b_1}{U_0} e_2^{b_2(u-U_0)};\ u < U_0, \end{cases}$$

where: b_1, b_2 – coefficients of approximation.

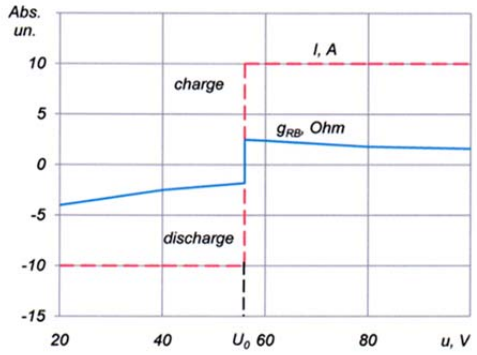

Fig. 4 Voltage-current characteristics of the battery

The first terms in these expressions represent horizontal but exponential sections of the VAC that provide a smooth transition between these areas along an almost vertical line, which corresponds to the regime's "charge-discharge" of a battery. Coefficient b_1 = 20 determines the marginal current of the battery; coefficient b_2 = 10 defines the degree of smoothing of the corners of the characteristic and the level of inclination from the vertical of the working area "charge-discharge" of a battery (it is selected experimentally). Thus, the generalized load resistance is determined by the equation:

$$(9)\qquad R_L = R_L(t,u) = \left(\frac{1}{r_L(t)} + \frac{1}{r_{BL}(u)} + g_{RB}(u) \right)^{-1},$$

where: r_L – resistance of payload (input impedance of the inverter).

A simplified mathematical description of the "rectifier-filter" node has the form:

$$(10)\qquad T_F \frac{du}{dt} + u = R_L I_L,$$

where: T_F – constant time filter,

$I_L = \sqrt{i_d^2 + i_q^2}$ – load current.

Charge q of the battery depends on its current and is described by the equation:

$$(11)\qquad T_{RB} \frac{du}{dt} = u g_{RB}(u),$$

where: T_{RB} – constant time characterizing the capacity of the battery, hence the speed of its charge and discharge.

The right side of the equation (11), battery current, is limited from the top and bottom at discharge and charge and is equal to zero: when the battery is discharged $u < U_0$; and when the battery is fully charged, and $u > U_0$.

Thus, equations (1) – (6) describe the mechanical dynamics of a WPI; equations (7), (1), and (7) – (9) describe the voltage u on the combined bus; equations (11) and (8) characterize the current battery charge.

Fig. 5 shows stationary schedules of a WPI at an interval of 70 seconds at random wind speed $V(t)$ varying from 8.4 to 13.5 m/s and the random nature of a change in load resistance $r_L(t)$ from 1.0 to 2.2 Ω, which corresponds to a fluctuation of the load power P_L from 1.8 to 3.0 kW. The calculation is based on the mathematical model described above, for WPI with a generator for constant neodymium magnets, whose design is patented by the authors of [7], with nominal power $P_{G.N}$ = 4 kW and the following numerical values of the parameters: inductance and phase resistance of the generator L_d = 0.0032 H, L_q = 0.0027 H, r = 0.3 Ω; the number of pole pairs p = 16; magnetic flux in the poles of permanent magnets Ψ = 0.165 Wb; coefficient of friction k_{cf} = 0.01; diameter of the wind wheel D = 4.6 m; moment of inertia of rotating masses J = 11.1 kg·m^2, time constants: T_{VD} = 1.1 s, T_{RB} = 20 s.

Fig. 5a depicts dependence of the basic mode parameters on time and Fig. 5b – on power. For clarity, the wind speed schedule is shown 5 times and the load resistance graph $r_L(t)$ is increased 10 times. The charts show WPIs in general successfully maintain voltage u on the combined bus at the level 56V. Small voltage deviations are only noticeable with significant differences in load resistance and wind speed. Thus, the voltage drop across the bus was in the range of 12.3s to 14s as a result of adverse effects of reducing the wind speed and load resistance, which led to a rapid discharge of the battery.

The graphs show that wind speed variation is accompanied by changes of the wind wheel moment which are explained by the inertia of the rotating masses WPI and require increased attention to the design of its mechanical part. At intervals of constant wind speed, the winder moment slightly exceeds the generator moment due to the presence of the friction moment. The speed of the generator tracks the change in wind speed with a delay due to the moment of inertia of the rotating masses and little depends on values of load resistance. The oscillator current experiences significant fluctuations, which is explained as a change in resistance $r_L(t)$ and $r_{BL}(t)$, and the current of the battery i_{RB} (Fig. 5; the charging current is accepted as positive and bit – negative). The battery charge is generally maintained at a sufficient level, except for the indicated case of voltage failure on the load, and in the range of 14s to 23s due to low load impedance.

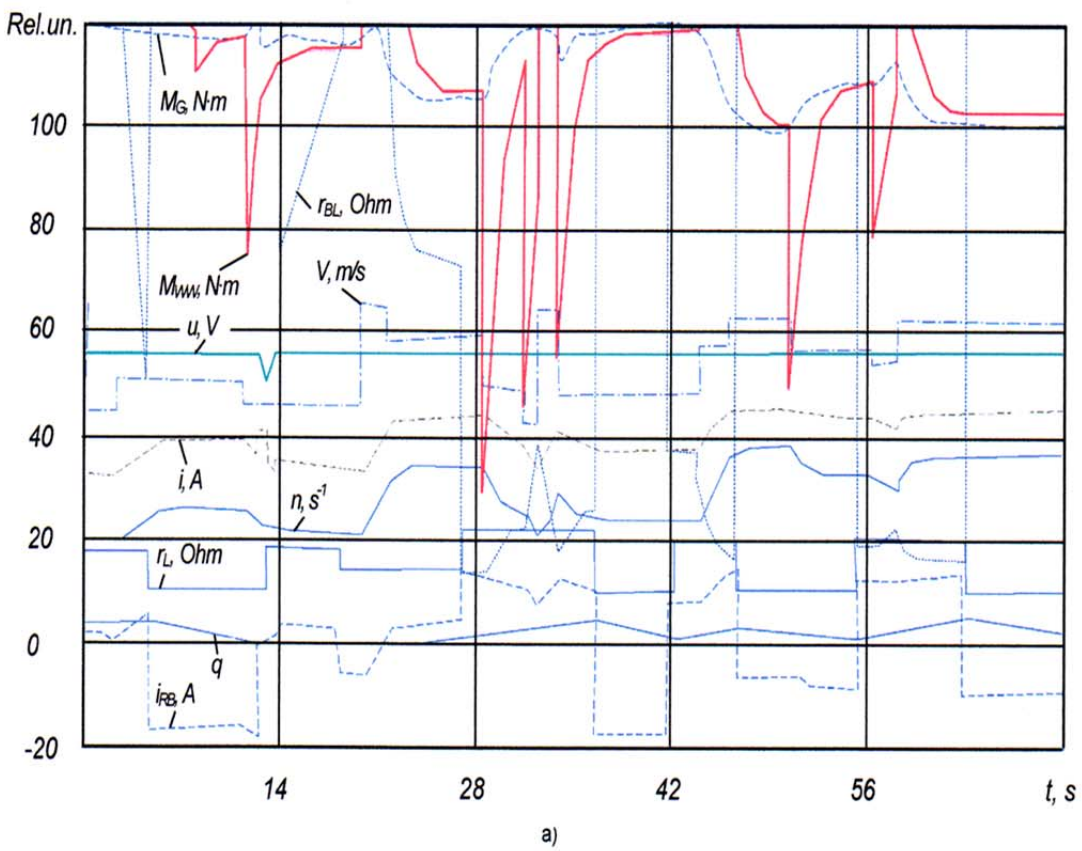

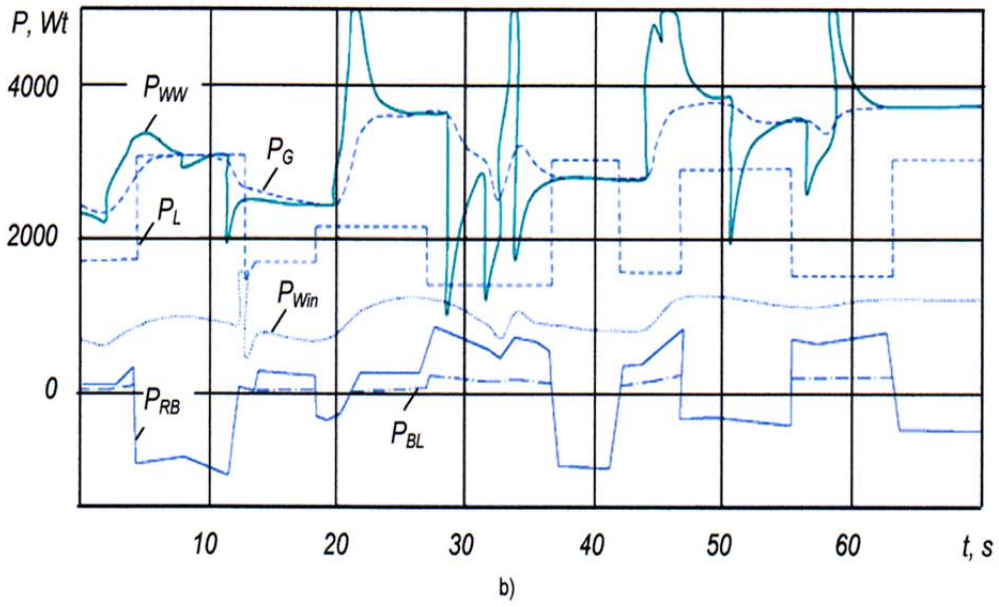

Fig.5. Stationary mode of the wind power installation

Power of the wind wheel $P_{WW}=\Omega \cdot M_{WW}$ (Fig. 5b) has sharp fluctuations according to wind speed variations. The power of the generator consists of load power, ballast resistance, the battery capacity, and power of generator windings. Due to the system inertia, the power of the generator $P_G = \Omega \cdot M_G$ changes smoothly and ranges from 2.5 kW to 3.7 kW. Since the voltage on the combined bus is virtually unchanged, the load graph $P_L(t)$ practically accurately repeats the schedule of change in load resistance $r_L(t)$. Battery capacity during the charge is positive and negative at the time of discharge, energizing the load at the power shortage of the generator. Fig. 5,b also illustrates load power $P_{BL}(t)$ and losses across the windings of the generator $P_{Win}(t)$.

Conclusion

The proposed functional scheme of the power supply system is based on low power WPI with a generator on permanent magnets. It provides a given voltage level on the assembly bus, and hence on the clamps of the load, with significant fluctuations in wind speed from 8.4 to 13.5 m/s and random variations of the load resistance, from 1.0 to 2.2 Ω, which corresponds to load power fluctuations from 1.8 to 3.0 kW.

The mathematical models adequately describe stationary and transitional regimes of WPI.

Non-direct wind turbines greatly improve overall dimensions and costs of the system.

A buffer battery of sufficient capacity, permanently attached to the load, provides a more stable WPI voltage in conditions of random of wind speed and load power oscillations.

***Authors**: Assistant Professor Mohamed Zaidan Qawaqzeh, Al-Balqa Applied University, E-mail: qawaqzeh@bau.edu.jo; dr inż. Andrzej Szafraniec, Kazimierz Pulaski University of Technology and Humanities in Radom, ul. Malczewskiego 29, 26-600 Radom, E-mail: a.szafraniec@uthrad.pl; Assistant Professor Serhii Halko, Tavria State Agrotechnological University, B. Khmelnitsky, 18, Melitopol, E-mail; galkosv@gmail.com; prof. dr hab. inż. Oleksandr Miroshnyk, Kharkiv Petro Vasylenko National Technical University of Agriculture, Alchevskyh, 44, Kharkiv, E-mail: omiroshnyk@ukr.net; ingineer Anton Zharkov, Tavria State Agrotechnological University, B. Khmelnitsky 18, E-mail: zharkov_victor@ukr.net.*

REFERENCES

[1] Yang Z., Chai Y., A survey of fault diagnosis for onshore grid-connected converter in wind energy conversion systems, *Renewable and Sustainable Energy Reviews*, 1 December 2016, Vol. 66, 345-359

[2] Gan L. K., Subiabre E., A realistic laboratory development of an isolated wind-battery system, *Renewable Energy*, Volume 136, 2019, 645-656

[3] Merizalde Y., Hernández-Callejo L., Duque-Perez O., Alonso-Gómez V., Maintenance models applied to wind turbines. A comprehensive overview, *Energies*, Vol. 12, Issue 2, 11 January 2019, 1-41

[4] Halko S.V., Zharkov V.Y., Zharkov A.V., Technologies and means of transformation of renewable energy sources for private households, *Melitopol Lux*, 2019, 215

[5] Twidell J., Weir. T., Renewable Energy Resources, Chapter 9, Power from the wind, *Taylor & Francis*, London and New York, 2006, 263- 323

[6] Zharkov V.Y., Chornenkyi V.Y., Novakh B.S., Zharkov A.V., Low-power low-power wind turbine generator, *Pat. 104467 UA. IPC F03D 7/06 (2006.01), F03D1/06 №201400015*, Published 10.02.2016, Bulletin №3

[7] Halko S.V., Novakh B.S., Zharkov A.V., Electric generator of flat design, *Pat. 116576 UA. IPC H02K21/00, H02K16/00, №201612745*, Published 25.05.2017, Bulletin №10

[8] Zharkov V.Y. Zhorov V.I., Zhorov S.V., Analysis of wind energy charge unit operation, *Scientific bulletin of Tavria State Agrotechnological University TSATU*, Melitopol, 2012, Vol. 2, №1

[9] Boubzizi S., Abid H., El Hajjaji A., Chaabane M., Comparative study of three types of controllers for DFIG in wind energy conversion system, *Protection and Control of Modern Power Systems*, Vol. 3, Issue 1, 1 December 2018.

[10] Siniscalchi-Minna S., Bianchi F.D., De-Prada-Gil M., Ocampo-Martinez C., A wind farm control strategy for power reserve maximization, *Renewable Energy*, Vol. 131, February 2019, 37-44

[11] Baran J., Jąderko A., Metoda śledzenia punktu mocy maksymalnej do sterowania turbiną wiatrową o regulowanej prędkości obrotowej, *Przegląd Elektrotechniczny,* nr 12/2019, 89-92

[12] Jąderko A., Mamok Ł., Odtwarzanie momentu aerodynamicznego mikroelektrowni wiatrowej w układzie sterowania z pełnym obserwatorem stanu, *Przegląd Elektrotechniczny,* nr 1/2020, 162-165

[13] Zharkov V.Y., Modern issues of household wind energy development, Proceedings of I Ukrainian scientitic and technical conference, *"DVNZ" DonNTU*, Donetsk, 2012, 127-128

[14] Bi H., Wang P., Wang Z., Common grounded H-type bidirectional DC-DC converter with a wide voltage conversion ratio for a hybrid energy storage system, *Energies*, Vol. 11, Issue 2, February 2018

[15] Komada P., Trunova I., Miroshnyk O. Savchenko O., Shchur T., The incentive scheme for maintaining or improving power supply quality, *Przegląd Elektrotechniczny,* nr 5/2019, 79-82

[16] Cetrini A., Cianetti F., Corradini M.L., Ippoliti G., Orlando G. On-line fatigue alleviation for wind turbines by a robust control approach, *International Journal of Electrical Power and Energy Systems*, Vol. 1, (9) 2019, 384-394

[17] Njiri J.G., Beganovic N., Do M.H., Söffker D. Consideration of lifetime and fatigue load in wind turbine control. *Renewable Energy*, Vol 131, 2019, 818-828